Available online at www.sciencedirect.com
ScienceDirect
Energy Reports 8 (2022) 835–846
www.elsevier.com/locate/egyr

2021 The 2nd International Conference on Power Engineering (ICPE 2021), December 09–11, 2021, Nanning, Guangxi, China

Output prediction of alpha-type Stirling engines using gradient boosted regression trees and corresponding heat recovery system optimization based on improved NSGA-II

Jiying Chen[a], Zedong Chu[b], Rui Zhao[a], Alexander F. Luo[c], Kai H. Luo[a,*]

[a] *Department of Mechanical Engineering, University College London, Torrington Place, London, WC1E 7JE, United Kingdom*
[b] *Department of Electronic and Electrical Engineering, University College London, Gower St, London, WC1E 6BT, United Kingdom*
[c] *Department of Statistical Science, University College London, Gower St, London, WC1E 6BT, United Kingdom*

Received 26 January 2022; accepted 20 February 2022
Available online xxxx

Abstract

Climate change is becoming a pressing global concern, and the search for new energy and energy recovery technologies is becoming a worldwide research imperative. The broad adaptability of the Stirling engine to a wide variety of heat sources makes it a promising technology for industrial waste heat recovery and solar thermal generation. The operation of the Stirling engine involves a multi-physical coupled process of heat transfer and mechanics as well as non-linear losses due to mechanical friction and gas charge leaking. Therefore, accurate prediction of Stirling engine power output through theoretical analysis is complex and costly. Emerging machine learning algorithms like Gradient Boosted Regression Trees (GBRT) can offer new approaches to solve this problem. The GBRT model consists of multiple decision trees that branch by exhausting thresholds for all features under study to find the best split structure for data regression, and the principle of GBRT gives it the natural advantage of finding a wide range of distinguishing features and combinations, and a powerful generalization capability. A GBRT forecasting model is thus constructed to model the output power of Alpha-type Stirling engines. Test data from the General Motors 4L23 Stirling Engine are applied as the training and test set. Results from the random test set accounting for 25% of the total samples indicate that the GBRT model has a prediction accuracy of 96.23%. Furthermore, a regional microgrid containing Stirling engines, photovoltaic panels and batteries for industrial waste heat recovery is constructed and an evaluation system for energy supply performance is also established. Finally, based on the proposed power output model, multi-objective optimization based on improved NSGA-II is implemented, providing guidance for industrial application of Stirling engines.

Peer-review under responsibility of the scientific committee of the 2021 The 2nd International Conference on Power Engineering, ICPE, 2021.

Keywords: Stirling engine; Output prediction; GBRT; Heat recovery system; Improved NSGA-II

* Corresponding author.
E-mail address: k.luo@ucl.ac.uk (K.H. Luo).

https://doi.org/10.1016/j.egyr.2022.02.244

Peer-review under responsibility of the scientific committee of the 2021 The 2nd International Conference on Power Engineering, ICPE, 2021.

1. Introduction

Stirling engines work by cyclic compression and expansion of the working fluid in an enclosure. As long as there is a temperature difference, the Stirling engine can convert thermal energy into mechanical works, which in turn can be converted into electricity. A wide variety of heat resources can be used, which makes a Stirling engine quite versatile. By the end of the 20th century, the twin problem of global energy shortage and climate change became increasingly acute, and countries worldwide were seeking for new energy resources and technologies. Driven by the urgent need for clean energy and industrial waste heat recovery, Stirling engines have experienced a tremendous development phase [1]. Its application range has been broadened to underwater power, waste heat recovery, and solar thermal power generation [2–4] and so on. Stirling engines' structures and thermodynamics states during operation are intricate. Typical research approaches for Stirling engines are ideal loss-free Schmidt analysis [5], adiabatic analysis [6], nodal analysis [7] and computational fluid dynamics modelling [8,9], also known as first-order, second-order, third-order and fourth-order design methods, respectively.

Over the last few decades, there has been a great deal of work on the thermodynamic modelling and experimental measurements of Stirling engines. Paula et al. indicated that the first-order model allows the performance parameters of the Stirling engine to be described, providing quick results with an accuracy of around 60% when calculating power [10]. Dobre et al. [11] established hybrid models using the finite physical dimension thermodynamics (FPDT) method and zero-dimensional modelling by the imperfectly regenerated Schmidt equation to develop analytical models for the Stirling engine cycle. Xiao et al. [12] proposed an approach to combine the second-order and third-order analysis methods for a 100 W beta-type Stirling engine optimization, taking advantage of the features of reliable accuracy and comprehensive operational information from the second-order and the third-order design methods, respectively. This study reached about 80% simulation accuracy. Hadi et al. [13] developed a new model called polytropic-finite speed thermodynamics (PFST). Its predicted thermal efficiency and power output of the GPU-3 Stirling engine had errors ranging from 2% to 34% in various operation conditions. Caetano et al. [14] proposed a novel fourth-order CFD model for beta-type Stirling engine transient simulation. The presented methodology combines first-order mathematical models with CFD simulations, reducing the error to around 2.6%. The accuracy of the analytical model usually decreases with the complexity of the problem. There are no models in the scientific literature that satisfactorily simulate the behaviour of real Stirling engines [14]. And computationally costly models are limited in terms of what they can be applied to [15].

To tackle the difficulties of uncertain relationship mapping of the thermodynamics parameters and the high cost of analytical calculations, emerging machine learning methods offer new ideas for solving these problems [16]. Machine learning is a technique for constructing problem-solving models from data. The process of extracting implicit and potentially useful information from data to be learned is called the model learning or training process [17]. Commonly used machine learning methods for regression and prediction include: naive Bayesian, decision tree, random forest, support vector machines, gradient decision trees, etc [18–20]. Gradient Boosted Regression Trees (GBRT) is one of the most effective machine learning prediction algorithms. It consists of multiple decision trees that can branch freely. The idea of GBRT gives it the natural advantage of finding multiple distinguishing features and combinations of features, and has a powerful generalization capability [21,22]. Unlike big data-driven models such as neural networks, GBRT has very high accuracy even with limited training data. Based on the above characteristics, the GBRT method is selected in this study to build a power output fuzzy model considering temperature, speed and pressure based on the test data of a commercial product of Stirling engines. The regression tree can be trained to perform reasonable threshold planning and bifurcation regression for several parameters affecting the performance of Stirling engines parallelly. Results on a random test set representing 25% of the total data showed an average accuracy of 96.23%. Furthermore, based on the power prediction model proposed, a microgrid containing Stirling engines, domestic photovoltaic panels and energy storage units is constructed, and an energy supply evaluation system that includes consideration of energy losses and fluctuations is also built. Based on the multi-objective optimization implemented by NSGA-II, a decision on the configuration of the energy system is finally proposed.

2. Alpha-type Stirling engine

According to the cylinder configuration, Stirling engines can be divided into three classifications, namely, alpha-type, beta-type, and gamma-type. The Alpha-type Stirling engine has two pistons providing the power output while

the Beta-type and Gamma-type Stirling engines both have only one piston to generate power. The engine under study is the General Motors 4L23 Stirling engine which is a compact multi-cylinder device composed of several Alpha-type Stirling engines in series to achieve high specific power output [23]. The configuration and main specifications of the General Motors 4L23 Stirling engine are displayed in Table 1 and Fig. 1.

Table 1. Core parameters of General Motors 4L23 Stirling engine.

Parameters	Description or Value
Working Fluid	Hydrogen
Inside Heater Tube Wall Temperature	649 °C
Inlet Cooling Water Temperature	57 °C
Engine speed	2000 rpm
Mean Pressure	1400 psia (9653 kPa)
Mechanical Efficiency	92%
Furnace Efficiency	85%
Cylinder Diameter	72 mm
Piston Stroke	48 mm
Inside Diameter of Pipes in Heater	5.0 mm
Length of Pipes in Heater	260 mm
Inside Diameter of Pipes in Cooler	1.0 mm
Length of Pipes in Cooler	120 mm

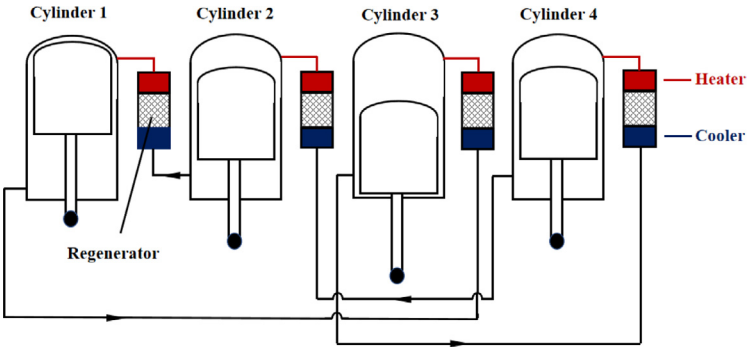

Fig. 1. Configuration schematic diagram for General Motors 4L23 Stirling engine.

3. Gradient Boosted Regression Trees (GBRT)

GBRT is a modification of the Boosting algorithm. In the original Boosting algorithm, each sample is assigned an equal weight value at the beginning of the algorithm, and initially all the base learners have the same importance. In GBRT, samples that are incorrectly predicted are given a higher weight in the next step, while samples that are correctly predicted are given a lower weight, helping the model to focus more on difficult samples and improving the performance of the model more efficiently. After N iterations have been performed, N simple base learners will be obtained. Finally, the resulting learners are combined and weighted (the larger the error rate the smaller the base decision tree weight value; vice versa, the smaller the error rate the larger the base decision tree weight value) to obtain a final model [24,25].

GBRT differs significantly from traditional Boosting in that each computation is designed to reduce the residuals from the previous one. In each iteration, the new decision tree is fitted to a subset of the original training set rather than to the residuals of the original training set, which is randomly sampled by no-relaxation of the original training set, similar to a self-sampling method. Each new decision tree is built so that the previous model residuals are reduced in the direction of the gradient, in contrast to the traditional Boosting algorithm which weights the correct and incorrect samples. Fig. 2 illustrates the general principle of the GBRT-Stirling engine output model proposed.

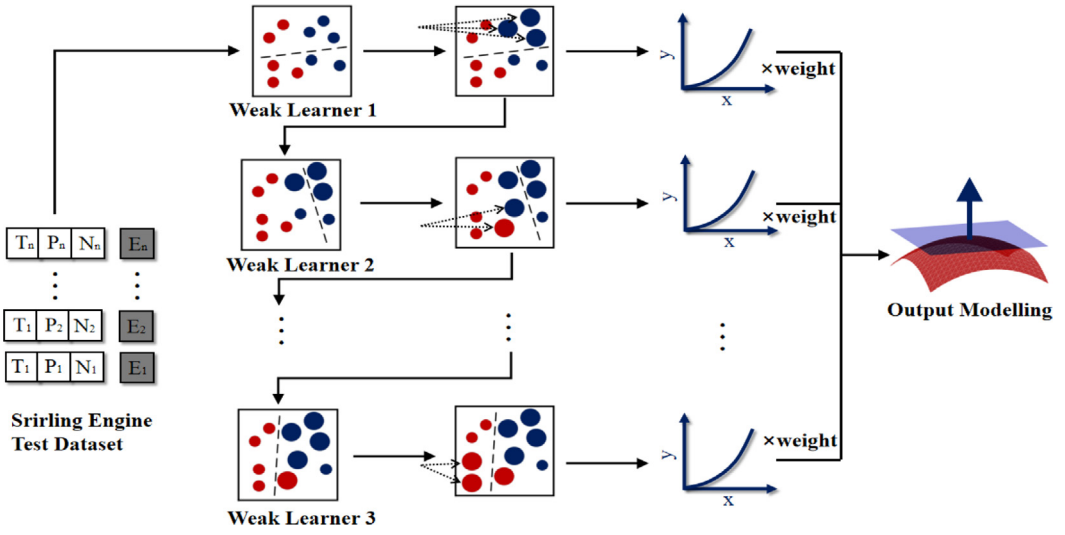

Fig. 2. Algorithm schematic for GBRT-based Stirling engine output prediction model.

Input:

$$\begin{cases}\vec{x}_i=(T_i,P_i,N_i)\\ \tilde{y}=(E_1,E_2,E_3,\cdots E_i)\end{cases}\qquad D=\left\{\left(\vec{x}_1,\tilde{y}_1\right),\left(\vec{x}_2,\tilde{y}_2\right),\cdots\left(\vec{x}_N,\tilde{y}_N\right)\right\},\vec{x}_i\in R^n,\tilde{y}_i\in R$$

$$loss\ \ function\ L=\left(\tilde{y},\hat{y}\right)=\min\sum_{i=1}^{N}\left[\tilde{y}_i,\hat{y}_i\right]^2$$

Output:

$$regression\ \ tree\ f_M\left(\vec{x}\right)$$

1. Initialization:

$$f_0(x)=\arg\min_{\rho}\sum_{i=1}^{N}L\left(\tilde{y}_i,\rho\right)\qquad g_m(x)=\sum_{j=1}^{J}\left(K_{m,j}I\right),x\in R_{m,j}\qquad I\left(x\in R_{jm}\right)=\begin{cases}1, & x\in R_{m.j}\\ 0, & x\notin R_{m.j}\end{cases}$$

2. For m=1,2, …, M

2.1 For i=1,2, ..., N

$$r_{i,m}=-\left[\frac{\partial L\left(\tilde{y}_i,f\left(\vec{x}_i\right)\right)}{\partial f\left(\vec{x}_i\right)}\right]_{f\left(\vec{x}\right)=f_{m-1}\left(\vec{x}\right)}$$

2.2 Fit a regression tree for $r_{j,m}$ to obtain the tree branch node region $R_{m,j}$ of the m-th tree

2.3 For j=1, 2, ..., J

$$\rho_{m,j}=\arg\min_{\rho}\sum_{i=1}^{N}L\left(\tilde{y}_i,f_{m-1}\left(\vec{x}_i\right)+\rho g_m\left(\vec{x}_i\right)\right)$$

2.4 Update $f_m\left(\vec{x}\right)=f_{m-1}\left(\vec{x}\right)+\gamma\sum_{j=1}^{J}\rho_{m,j}g_m\left(\vec{x}\right),\vec{x}\in R_{m.j}$

3. Final Regression Tree Model: $f_M\left(\vec{x}\right)=\sum_{m=1}^{M}\sum_{j=1}^{J}\rho_{m,j}I\left(\vec{x}\in R_{m.j}\right)$

The measured temperature, pressure and speed data from the Stirling heat engine under study can form a vector space, and the output power or efficiency can form a one-dimensional column vector.

$$\begin{cases} \overrightarrow{x_i} = (T_i, P_i, N_i) \\ \tilde{y} = (E_1, E_2, E_3, \ldots, E_i) \end{cases} \tag{1}$$

For regression prediction problems, the squared error loss function is usually chosen as follows:

$$L = (\tilde{y}, \hat{y}) = (\tilde{y} - \hat{y})^2 \tag{2}$$

The input data set is $D = \{(x_1, y_1), (x_2, y_2), \ldots, (x_N, y_N)\}$. L denotes the loss function. M represents the number of regression trees. And Y represents the learning rate. J denotes each regression tree's branch nodes. Input space is partitioned into J disjoint regions $R_{m,1}$, $R_{m,2}$, ..., $R_{m,j}$, and initial constants K are estimated for each region at the beginning. Our algorithm is able to freely exhaust the ideal regression model in the temperature–pressure–speed vector space. The complete construction processes are as follows.

4. Power output prediction

The initial value of the number of regression trees is set to 100 and the overall learning rate is set to 0.1. The Stirling engine under study is tested 240 times in the temperature ranging from 1000 to 1500 K, pressure ranging from 500 to 2500 psia and speed ranging from 500 to 3000 rpm. 25% experimental data are selected as the test set and the remaining points are used as the training set. Results of the GBRT-Stirling Engine output prediction are shown in Fig. 3. On the random test set, which never appeared in the training set, there is a high match between the GBRT model and the actual data. Fig. 4 visualizes the performance of the algorithm in terms of accuracy. Residual diagram in Fig. 4 shows that the majority of test points have residual values below 5%. To be precise, the model proposed has an average prediction accuracy of 96.23%. Furthermore, the output model containing multiple operation parameters is presented by the way of spatial power surfaces. Spatial curved surfaces in Figs. 5 and 6 are the pressure-engine speed-output and temperature-engine speed-output obtained by GBRT, separately. Power surfaces are usually smooth and show a certain regularity. In addition to power, cycle efficiency is also critical to engine operation. Since the general GBRT model only allows a single output, power and efficiency cannot be export simultaneously. Therefore, replacing the training target from power output to efficiency, Fig. 7 illustrates the efficiency performance of the studied Stirling engine constructed by GBRT under a wide range of operating conditions. Fig. 7 indicates that the efficiency is more sensitive to changes in operating conditions, but also shows a roughly regular pattern containing areas of stable efficiency and areas of sudden increase. The mapping relationship between multiple operation parameters and output performance is finally established.

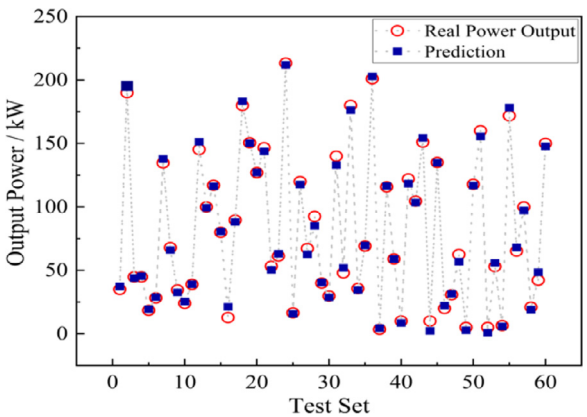

Fig. 3. Performance of GBRT on the test set.

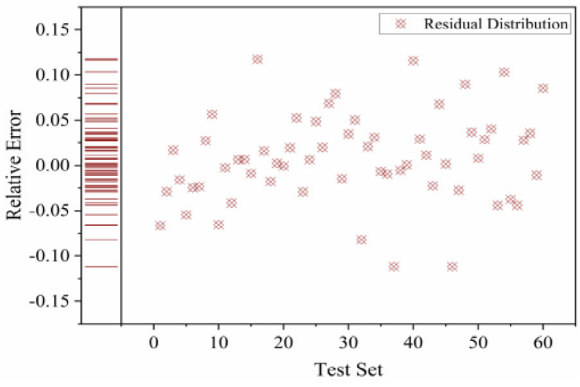

Fig. 4. Residual values and distribution.

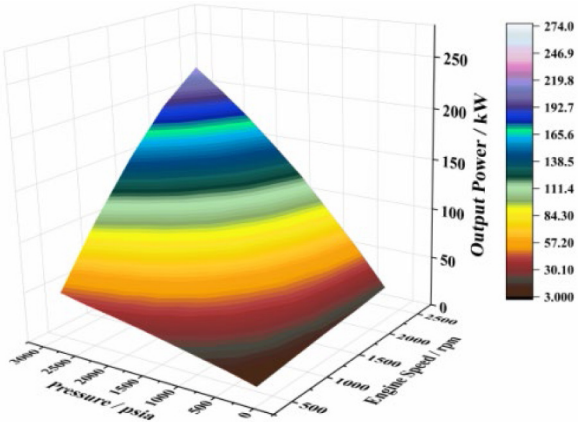

Fig. 5. Pressure-speed-output spatial surface.

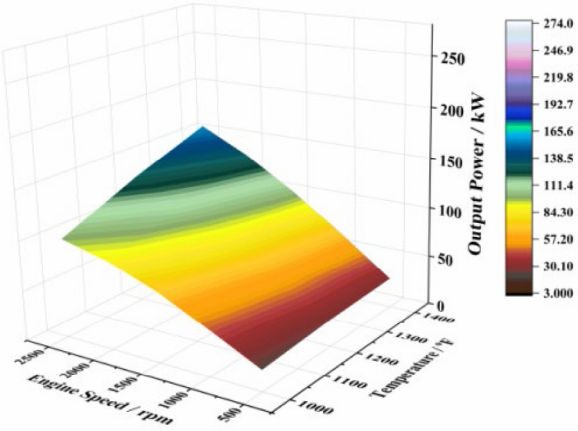

Fig. 6. Surface plot for Temperature–speed versus output.

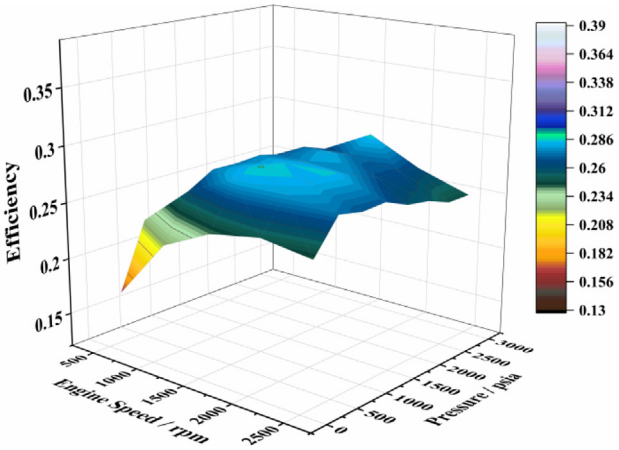

Fig. 7. Curved surface of output efficiency constructed by GBRT prediction results.

5. Case study

5.1. Stirling– PV microgrid

After obtaining the output model, a Stirling engine–Photovoltaic microgrid located in the suburban area of London is constructed in Fig. 8. This system mainly consists of Stirling engines array, generators, rooftop PV panels, storage units and the control centre. Stirling engines and PV panels are power resources. A comprehensive list of end-users containing industry parks, shopping malls and resident communities is selected as the energy consumers (Fig. 9). Based on the collected annual load curves, it is clear that the different energy consumers show different seasonal characteristics and fluctuations. The integrated energy consumers used for the case study are representative and have a considerable research value. Figs. 10 and 11 illustrates the annual solar incident data in London and the temperature of fuel gas from a thermal plant which is used for Stirling engine waste heat recovery, respectively. Power generated by the Stirling engine can be obtained as follows:

$$P_{SE}(t) = GBRT(T_{waste}, p, N)_t \times \eta_{syn} \tag{3}$$

where T_{waste} denotes the temperature of waste heat resources, η_{syn} denotes the synchronous motor efficiency which is equal to 96% in this case. The electric power generated by the rooftop PV panel (P_{PV}) is mainly determined by the solar spectrum wavelength, absorptivity, and aperture areas. The rating power is 0.325 kW with the PV efficiency of 16.94% [26,27].

$$T_{PV} = T_{amb} + (T_{nor} - T_{amb}) \times \frac{G(t)}{I_{solarradiation}} \tag{4}$$

$$P_{PV}(t) = G(t) \times P_{PV-STC} \times r_{PV} \times [1 - \beta (T_{PV} - T_{PV-STC})] \tag{5}$$

where T_{PV} indicates the PV operation temperature while T_{nor} and T_{amb} represent the normal operation temperature and ambient temperature, respectively. I denotes the irradiance on cell surface, which is equal to 800 W/m^2. $G(t)$ denotes the incident solar irradiation; $P_{\mathrm{PV-STV}}$ and r_{PV} are the power under the standard test condition and the power reduction coefficient, respectively. β is the PV temperature coefficient.

5.2. System evaluation

For the constructed Stirling–PV microgrid, evaluation indicators are required as the objective function for conducting multi-objective optimization. This study focuses on considering the performance of the energy system and therefore starts with both energy losses and energy fluctuations. In order to reduce the excessive power losses caused by overload generation and to improve the energy efficiency of the system, the coefficient of energy loss (CEL) is introduced

$$P(t) = P_{SE}(t) + P_{PV}(t) + P_{bat}(t) - P_{load}(t) \tag{6}$$

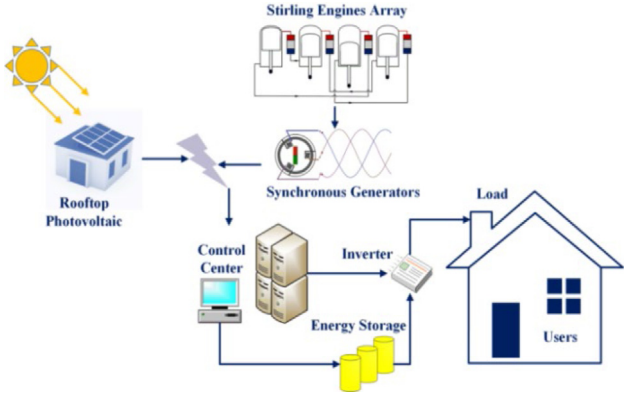

Fig. 8. Stirling engine–PV integrated microgrid.

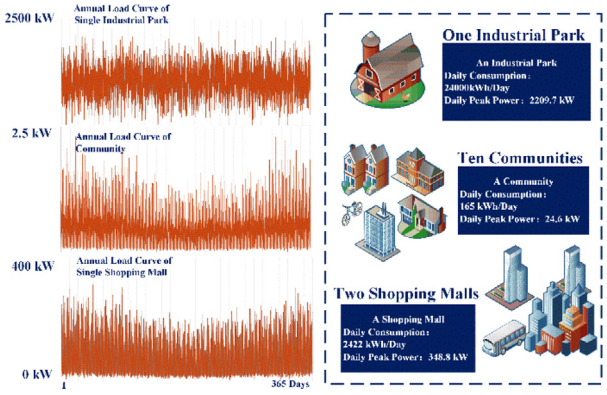

Fig. 9. Selected comprehensive power consumption community.

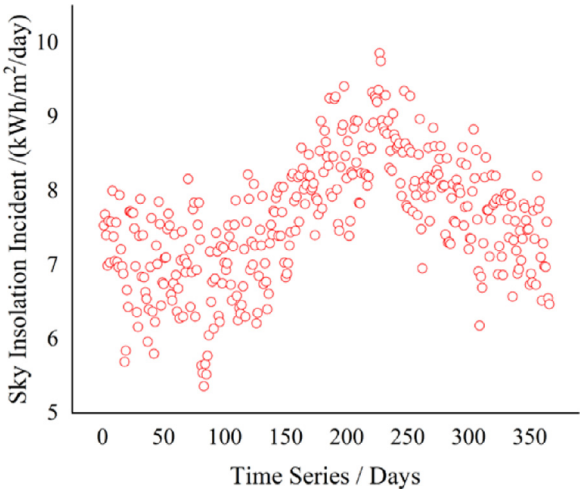

Fig. 10. Annual sky insolation incident.

$$CEL = \frac{\sum_{t=1}^{n} [P(t) - P_{bat}(t-1)]}{\sum_{t=1}^{n} [P_{SE}(t) + P_{PV}(t)]} \tag{7}$$

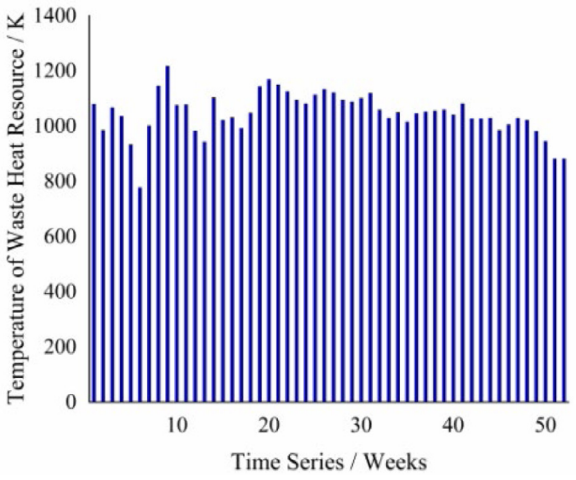

Fig. 11. Temperature profile of heat resources for waste heat recovery.

where P(t) represents the mismatch between the power generation from the Stirling engine, PV panels and the user's energy demands. n is equal to 8760, this is because the planning time window is one year, which is treated as 8760 h. A well-organized energy system also needs to enable the output power to be well matched to the consumer load and avoid excessive fluctuations throughout the system. The optimization of the system with regard to energy supply fluctuations is essential. In view of this, the coefficient of historical volatility (CHV) is established to evaluate the system's stability.

$$u_t = \ln \frac{P(t)}{P(t-1)} \quad CHV = \sqrt{\frac{1}{n-1}\sum_{i=1}^{n}(u_i - \overline{u})} \tag{8}$$

5.3. Improved Non-dominated Sorting Genetic Algorithm-II (NSGA-II)

NSGA-II, proposed by Kalyanmoy Deb in 2002 [27], is one of the most commonly used optimization approaches in multi-objective problem (MOP). This algorithm with operator improvements is selected to conduct configuration optimization on the proposed Stirling–PV microgrid. Before further improvements can be made, the characteristics of NSGA-II need to be elaborated. At the initial stage of population evolution, where the similarity of population individuals is low, increasing the crossover probability will accelerate the population evolution, while reducing the variation probability of the population will reduce the tedious computational process. In the middle stage of evolution, increasing the variation probability will prevent the iteration of the algorithm from falling into local optimum. In the final stage of evolution, individuals are very similar. And the crossover probability and variation probability should be reduced in order to achieve the gradual convergence of the algorithm [28]. The operators for crossover and variation will be improved by adaptation so that they are similar to the above trends. The improvements of the operators are formulated as equations for P_c and P_M, respectively.

$$P_c = \frac{1}{2}\cos\left(\frac{\pi t_i}{2S}\right) \tag{9}$$

$$P_M = \frac{1}{\tau\pi\left[1 + \left(\frac{t_i - kS}{\tau}\right)^2\right]} \tag{10}$$

where S denotes the maximum number of generations, t_i is the current generation number (0<i<S), τ is the scale parameter which specifies the half-width at half-maximum, k is the coefficient that divides the total number of generations is equal to 0.5 in this case. The flow chart for NSGA-II is displayed in Fig. 12. Detailed description for the framework and principle of NSGA-II can be found in the literature [27]. The variable in the optimization is

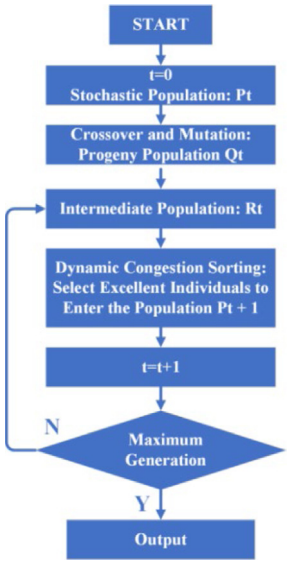

Fig. 12. Flow chart for NSGA-II.

the configuration of the energy system, specifically the installed capacity of the Stirling engines and photovoltaic panels for the current user. After about 200 generations, the energy system under study has reached a common compromise on the two proposed evaluation indicators (see Table 2).

Table 2. Optimal energy system configuration.

Energy Supply	Installation Number	CEL	CHV
Stirling Engine (250 kW)	10	0.2384	0.3931
PV Panel (0.325 kW)	1727		

Through multi-objective optimization, the performance of the energy system studied is significantly improved. The figure for CEL is reduced to 0.231, which means that there is a higher degree of matching between the load and the power supply. In addition, the figure for CHV is reduced to 0.392, implying that the system history fluctuations have been eliminated considerably and the energy stability has been significantly enhanced (see Fig. 13).

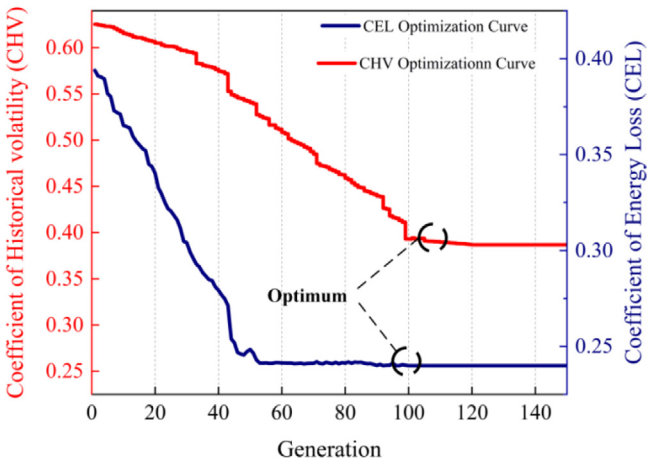

Fig. 13. Performance on the energy loss and fluctuation during optimization.

6. Conclusion

In this work, a practical and accurate approach through GBRT to enable Stirling engines performance prediction is proposed. Taking the experimental data of a commercial product as the example, the mapping relationship between operation parameters (temperature, pressure and engine speed) and output performance is constructed accurately. Furthermore, a Stirling engine–PV microgrid is designed to power a specific energy consumption community. An improved NSGA-II multi-objective optimization algorithm is developed to further improve the proposed system's energy supply performance. The main research findings can be summarized as follows:

(1) The critical operation parameters of Stirling engines are used to form a vector space and acted as the input. The GBRT model is implemented to establish the mapping modelling between input vector space and the output vector. The input space is freely divided into disjoint regions and the branch points, and thresholds that can minimize the residuals are explored by 100 regression trees, resulting in the optimal Stirling engine operation model. Results on the random test set indicate that the average prediction accuracy can reach 96.23%.
(2) A Stirling-solar microgrid is further developed and a comprehensive evaluation model, considering both historical volatility and energy loss coefficients, is also proposed. Aiming to power a specific energy consumption community, an application of Stirling engine heat recovery on practical power supply is attempted.
(3) Through the multi-optimization by the improved NSGA-II method, the objective functions related to energy losses and stability achieve their optimum. Deep energy complementarity between generation and demand is finally obtained, providing guidance for industrial promotion and commercialization of Stirling engines.

Declaration of competing interest

The authors declare that they have no known competing financial interests or personal relationships that could have appeared to influence the work reported in this paper.

Acknowledgement

Support from the UK Engineering and Physical Sciences Research Council (EPSRC) under the project "Exascale Computing for System-Level Engineering: Design, Optimisation and Resilience" (Grant No. EP/V001531/1) is gratefully acknowledged.

References

[1] Li Zhi, Lu Yiji, Huang Rui, Chang Jinwei, Yu Xiaonan, Jiang Ruicheng, Yu Xiaoli, Roskilly Anthony Paul. Applications and technological challenges for heat recovery, storage and utilisation with latent thermal energy storage. Appl Energy 2021;283:116277, 2021.
[2] Hafez AZ, Soliman Ahmed, El-Metwally KA, Ismail IM. Solar parabolic dish stirling engine system design, simulation, and thermal analysis. Energy Convers Manage 2016;126:60–75, 2016.
[3] Li Daijin, Qin Kan, Luo Kai. Underwater striling engine design with modified one-dimensional model. Int J Nav Archit Ocean Eng 2015;7(3):526–39, 2015.
[4] Güven Metin, Bedir Hasan, Anlaş Günay. Optimization and application of stirling engine for waste heat recovery from a heavy-duty truck engine. Energy Convers Manage 2019;180:411–24, 2019.
[5] Erol Derviş, Yaman Hayri, Doğan Battal. A review development of rhombic drive mechanism used in the stirling engines. Renew Sustain Energy Rev 2017;78:1044–67, 2017.
[6] Ahadi Fatemeh, Azadi Mohammad, Biglari Mojtaba, Madani Seyed Navid. Study of coating effects on the performance of stirling engine by non-ideal adiabatic thermodynamics modeling. Energy Rep 2021;7:3688–702, 2021.
[7] Karabulut H, Yücesu HS, Çinar C. Nodal analysis of a stirling engine with concentric piston and displacer. Renew Energy 2006;31(13):2188–97, 2006.
[8] El-Ghafour SA, El-Ghandour M, Mikhael NN. Three-dimensional computational fluid dynamics simulation of stirling engine. Energy Convers Manage 2019;180(2019):533–49.
[9] Xiao Gang, Sultan Umair, Ni Mingjiang, Peng Hao, Zhou Xin, Wang Shulin, Luo Zhongyang. Design optimization with computational fluid dynamic analysis of β-type stirling engine. Appl Therm Eng 2017;113:87–102, 2017.
[10] Paula RB, Gonçalves JL, Cobas VRM, Lora EES. Theoretical assessment of a stirling engine 'amazon' by using prosa and mathcad. Rev Engenharia Térmica 2011;10:32–7, 2011.
[11] Dobre Cătălina, Grosu Lavinia, Costea Monica, Constantin Mihaela. Beta type stirling engine. Schmidt and finite physical dimensions thermodynamics methods faced to experiments. Entropy 2020;22(11):1278, 2020.

[12] Xiao Gang, Huang Yiqing, Wang Shulin, Peng Hao, Ni Mingjiang, Gan Zhihua, Luo Zhongyang, Cen Kefa. An approach to combine the second-order and third-order analysis methods for optimization of a stirling engine. Energy Convers Manage 2018;165(2018):447–58.
[13] Hosseinzade Hadi, Sayyaadi Hoseyn, Babaelahi Mojtaba. A new closed-form analytical thermal model for simulating stirling engines based on polytropic-finite speed thermodynamics. Energy Convers Manage 2015;90(2015):395–408.
[14] Caetano Bryan Castro, Lara Isadora Figueiredo, Borges Matheus Ungaretti, Sandoval Oscar R, Valle Ramón Molina. A novel methodology on beta-type stirling engine simulation using CFD. Energy Convers Manage 2019;184(2019):510–20.
[15] Zhu Shunmin, Yu Guoyao, O. Jongmin, Xu Tao, Wu Zhanghua, Dai Wei, Luo Ercang. Modeling and experimental investigation of a free-piston stirling engine-based micro-combined heat and power system. Appl Energy 2018;226(2018):522–33.
[16] Ning Chao, You Fengqi. Optimization under uncertainty in the era of big data and deep learning: When machine learning meets mathematical programming. Comput Chem Eng 2019;125(2019):434–48.
[17] Ghoddusi Hamed, Creamer Germán G, Rafizadeh Nima. Machine learning in energy economics and finance: A review. Energy Econ 2019;81(2019):709–27.
[18] Yager Ronald R. An extension of the naive Bayesian classifier. Inform Sci 2006;176(5):577–88, 2006.
[19] Paul Angshuman, Mukherjee Dipti Prasad, Das Prasun, Gangopadhyay Abhinandan, Chintha Appa Rao, Kundu Saurabh. Improved random forest for classification. IEEE Trans Image Process 2018;27(8):4012–24, 2018.
[20] Nalepa Jakub, Kawulok Michal. Selecting training sets for support vector machines: A review. Artif Intell Rev 2018;52(2):857–900, 2018.
[21] Zhang Zhendong, Jung Cheolkon. GBDT-MO: Gradient-boosted decision trees for multiple outputs. IEEE Trans Neural Netw Learn Syst 2021;32(7):3156–67, 2021.
[22] Persson Caroline, Bacher Peder, Shiga Takahiro, Madsen Henrik. Multi-site solar power forecasting using gradient boosted regression trees. Sol Energy 2017;150:423–36, 2017.
[23] Jiang Han, Xi Zhongli, Rahman Anas A, Zhang Xiaoqing. Prediction of output power with artificial neural network using extended datasets for stirling engines. Appl Energy 2020;271(2020):115123.
[24] Biau G, Cadre B, Rouvière L. Accelerated gradient boosting. Mach Learn 2019;108(2019):971–92.
[25] Torres-Barrán Alberto, Alonso Álvaro, Dorronsoro José R. Regression tree ensembles for wind energy and solar radiation prediction. Neurocomputing 2019;326–327:151–60, (2019).
[26] Martin N, Ruiz JM. Calculation of the PV modules angular losses under field conditions by means of an analytical model. Sol Energy Mater Sol Cells 2001;70(1):25–38, 2001.
[27] Deb K, Pratap A, Agarwal S, Meyarivan T. A fast and elitist multiobjective genetic algorithm: NSGA-II. IEEE Trans Evol Comput 2002;6(2):182–97, 2002.
[28] OuYang J, Yang F, Yang SW, Nie ZP. The improved NSGA-II approach. J Electromagn Waves Appl 2008;22(2008):163–72.